NO Bonding to Heme Groups: DFT and Correlated ab Initio Calculations

Julianna Oláh and Jeremy N. Harvey*

Centre for Computational Chemistry, School of Chemistry, University of Bristol, Cantock's Close, Bristol BS8 1TS, U.K.

Received: December 22, 2008; Revised Manuscript Received: March 13, 2009

The accuracy of DFT methods for treating NO bonding to heme groups, both with ferric and ferrous iron, is assessed. These systems are shown to be unusually challenging for obtaining accurate binding energies. The hybrid functionals B3LYP and B3PW91 underestimate the bond energy, and the nonhybrid functional BP86 overestimates it as well as predicting the wrong energy ordering for the different spin states of the heme group prior to NO bonding. Large basis set CCSD(T) calculations on model complexes confirm that B3LYP and B3PW91 underestimate the bond strength for NO, by ca. 10 kcal/mol. This is suggested to be due to an underestimate of the medium-range electron correlation associated with metal−ligand π bonding in this system.

1. Introduction

The binding of small ligands such as O_2, CO, H_2O, and NO to metalloproteins[1] and to transition metal complexes[2] has received a lot of attention due to the important biological role of these molecules. There is significant value in using computational methods to predict and rationalize the thermochemistry of ligand binding as well as the kinetics. However, the challenges involved in calculating these properties accurately are significant. We have previously carried out DFT calculations aimed at understanding reactivity in addition of CO to a heme group containing an Fe(II) center, taking into account the effect of spin-state change during the addition.[3] We have also carried out hybrid quantum-mechanical/molecular mechanics (QM/MM) calculations, again using DFT for the QM region, addressing the thermochemistry of CO addition to the Fe(II) heme group in myoglobin.[4]

More recently, we carried out a comparative study[5] of the mechanism and thermochemistry of bonding of CO and H_2O, as well as NO and O_2, to model systems of Fe(II) porphyrins. As part of this study, we sought to evaluate how accurate popular DFT functionals are in describing the energetics of the different spin states and of the ligand addition, by carrying out benchmark CCSD(T) calculations on small models. This work showed that hybrid functionals, such as the B3LYP and B3PW91 functionals, describe the bonding of CO and H_2O to Fe(II) porphyrins adequately, as they are in good agreement with CCSD(T) results for model systems. However, due to the low symmetry of the NO and O_2 adducts, we were unable to explore the performance of DFT in describing the bonding of NO and O_2 to heme systems by comparing the data to CCSD(T) results. The calculated DFT results for O_2 seem roughly to agree with experiment, as discussed by other authors;[6] however, the NO bond energies for model Fe(II) porphyrin (FeP(Im), see Figure 1) systems calculated by hybrid DFT functionals seem to be rather low when compared to experiment.

The coordination of NO to hemoproteins and model Fe(II/III) systems has been recently reviewed.[7] In general Fe(II) porphyrins show slightly larger association rate constants for binding of NO than Fe(III) systems, but the equilibrium in all cases is strongly shifted into the direction of complex formation. Of particular interest to us is the binding of NO to P450cam[8] and to a synthetic heme−thiolate complex,[9] as it gives information on the general mechanism of binding of NO to cytochrome P450s. In both cases laser flash photolysis and high-pressure stopped-flow kinetics have been used to obtain kinetic data and to elucidate the reaction mechanism. The common characteristic of all cytochrome P450s is a thiolate-ligated heme group, whose oxidation state and coordination characteristics change during the catalytic cycle of the enzyme. In ferric P450cam in the absence of camphor, the natural substrate of the enzyme, a water molecule is bound to the sixth distal position of the iron. Therefore, during the reaction with NO, the water ligand must be displaced before the coordination of NO can occur. The kinetic measurements showed the reaction energy for substitution of H_2O by NO has a reaction heat of −7.5 kcal/mol in the case of ferric P450cam. Interpreting this value in terms of a heme−NO bond energy is not straightforward, as one must account for the enthalpy of heme-H_2O bond breaking. However, when camphor is present, the heme iron center is only five-coordinate in the absence of NO, and spectroscopic arguments suggest that the camphor does not significantly affect the binding of NO. Hence the measured heat of reaction, of −20 kcal/mol, can be directly translated into a bond enthalpy of 20 kcal/mol.[8]

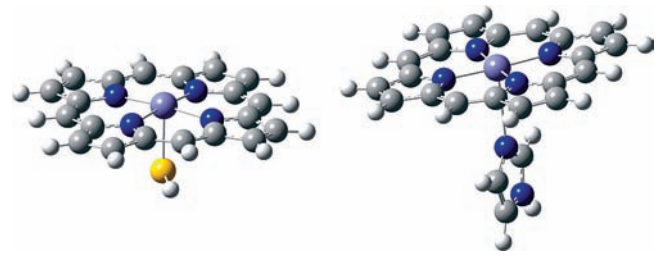

Figure 1. Molecular structures of FeP(SH) and FeP(Im).

Recently a synthetic heme−thiolate complex was shown to possess similar NO binding characteristics as most P450s.[10] From the equilibrium constant of the NO binding and dissociation reactions a Gibbs free energy of binding of −6.5 kcal/mol was measured at 5 °C. The Gibbs free energy of binding includes the effect of entropy changes, which are almost always significantly unfavorable toward ligand binding, with $-T\Delta S$ of

† Part of the "Robert Benny Gerber Festschrift".

* Corresponding author, jeremy.harvey@bris.ac.uk.

10.1021/jp811316n CCC: $40.75
Published on Web 04/08/2009

the order of 10 kcal/mol, so that the measured free energy of binding suggests, here too, a significantly negative enthalpy of binding, of the order of −15 kcal/mol or higher.

The binding energy of NO to cationic Fe(II/III) porphyrin systems has been measured in the gas phase, and on average binding enthalpies of ca. 25 kcal/mol have been reported.[11] In another study small ligand binding to cationic Fe(III)−heme$^+$ systems has been investigated.[12] NO showed exceptionally high affinity for Fe(III)−heme despite its low gas-phase basicity, and a binding free energy of 16 kcal/mol has been measured. As argued above, entropic effects are unfavorable for NO binding, so the bond enthalpy associated with this gas phase experiment should be larger, of the order of 25 kcal/mol, consistent with the other experimental values. Note that in these gas phase systems, contrary to what is found in enzymes, the heme iron is only pentacoordinate in the NO complexes, and tetracoordinate in the heme fragment prior to NO bonding.

There have been numerous computational studies on binding of NO to Fe(II/III) porphyrines. These include QM studies on model complexes as well as QM/MM studies addressing the chemistry in a given protein system.[13] Blomberg et al.[6] studied the binding of O_2, NO, and CO to bare porphyrins, models of myoglobin, and cytochrome *c* oxidase using the popular B3LYP functional. It was found that the Gibbs bond free energy for CO in these systems could be accurately described (e.g., for myoglobin the calculated bond free energy is 6.2 kcal/mol vs the value of 8.9 kcal/mol estimated from experiment), but for O_2 and especially NO much larger discrepancies were observed. For example, for myoglobin and O_2 a bond free energy of 12.8 kcal/mol was estimated from experiment, vs the calculated value of 2.8 kcal/mol. For both NO and O_2 the calculated results were about 10 kcal/mol lower than the experimental values. In the case of the O_2 adduct, it appears that stabilizing hydrogen bonds in the protein, absent in the model calculations, may account in part for the discrepancy,[14] but this effect is less important for NO.[6,15] On the other hand, pure DFT functionals seem to overestimate the NO−Fe(II) porphyrin bond strength. Parrinello et al. used the BP86 functional to study the addition of NO to bare Fe(II) porphyrin (FeP) and FeP imidazole (Im) systems.[16] For both cases, the BP86 functional predicted a bond energy for NO of about 35 kcal/mol, suggesting that the axial imidazole ligand does not influence the binding energy of NO. It should be noted that the BP86 method predicts a triplet ground state for both FeP and FeP(Im); this is in agreement with experiment in the former case but not the latter.

For the heme system with an Fe(II) center, a recent study compares DFT and CASSCF and CASPT2 calculations, for binding of O_2, CO, and NO.[17] On the basis of the CASPT2 results, this study concludes that functionals such as B3LYP underestimate the bond energy for binding of all three small ligands. This differs somewhat from our conclusion, derived from CCSD(T) calculations, that B3LYP performs acceptably for the CO adduct,[5] but it is noteworthy that the CASPT2 calculations suggest that the error with B3LYP is most severe in the case of NO, at close to 20 kcal/mol, so clearly this case is problematic.

Given the significant experimental interest in NO−heme adducts, due to their possible role in cell signaling, regulation of metabolism, and other aspects of biochemistry, a large number of other DFT studies, both on small models[18] and on whole proteins (using hybrid QM/MM methodology),[13] have addressed NO binding. The discussion above suggests that it would be desirable to assess whether the deficiencies discussed above are indeed due to inaccuracy of the DFT methods or instead arise as a consequence of truncation to model systems. There is increasing interest in carrying out benchmark ab initio calculations with large basis sets[19] for bioinorganic systems.[20] In the specific area of binding of small ligands to heme groups, as well as our CCSD(T) work for CO and H_2O binding, the already mentioned recent CASPT2 study of binding to the full FeP(Im) system should be highlighted,[17] as this also includes NO binding, albeit only to Fe(II) systems.

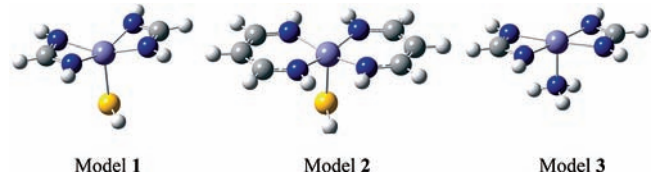

Figure 2. Molecular structure of model systems.

We here extend our previous CCSD(T) study to binding of NO, and consider models not only of the Fe(II) heme group but also of the Fe(III) center as found in cytochrome P450s. The present paper is organized as follows. After the computational details we briefly introduce the nature of the studied porphyrin systems and the electronic structure of the NO adducts. Then we describe the results of DFT calibration on model systems to CCSD(T) relative energies and NO-binding energies. An attempt is made to rationalize the deficiencies of the DFT results.

2. Computational Details

DFT calculations on the FeP(SH) and FeP(Im) systems (Figure 1) and on the models **1**, **2**, and **3** (Figure 2) were carried out with the Jaguar electronic structure package.[21] Geometries were optimized using the hybrid B3PW91 functional and the basis set combination BS I described below. Single-point calculations using several DFT functionals available in Jaguar 06 were carried out on all systems at the optimized B3PW91 geometry. The results obtained with the two typical hybrid functionals, B3PW91 and B3LYP, and a typical "pure" functional, BP86, are presented in the paper, with the results obtained using the other functionals given in Table S1in the Supporting Information. A restricted or restricted open-shell formalism was used throughout. In all these DFT calculations, the standard Los Alamos ECP with the Jaguar triple-ζ basis (LACV3P) was used for Fe, and the 6-31G(d) basis was used for all other atoms. In the rest of the paper we will refer to this basis set combination as BS I. For these calculations pseudospectral grids were used throughout.

The single-point CCSD and CCSD(T) energies for models **1**,**2**, and **3** were computed at the previous B3PW91 geometries, using the MOLPRO2006.3[22] program package. One-electron integrals were computed using a Douglas−Kroll method; hence the calculations incorporate relativistic effects at least approximately. The calculations were performed using the Douglas−Kroll recontraction[23] of the cc-pVDZ, cc-pVTZ, and cc-pVQZ basis sets by Dunning et al.[24] for H, C, N, O, and S atoms. For iron we used the cc-pVTZ and cc-pVQZ basis sets developed by Balabanov and Peterson, also in forms adapted for use with Douglas−Kroll one-electron integrals.[25] For extrapolation to the infinite basis set limit, we used the same strategy as in our previous work to make the calculations computationally feasible.[5] We divided the molecules into two parts: part I consisted of the iron atom and the NO ligand, if present, while the amidines and the SH ligand in the case of models **1** and **2** and the NH_3 ligand for model **3** formed part II. Part I was described using the larger cc-pVTZ and cc-pVQZ

basis sets, whereas in most of the calculations the description of part II was restricted to the cc-pVDZ basis set. To investigate whether the smaller basis set used on the atoms of part II introduced unacceptable errors, some additional calculations were carried out for model **1** using the cc-pVTZ basis set on the atoms of part II. The obtained results indicated that usage of the cc-pVDZ and cc-PVTZ basis sets on the atoms of part II lead to only minor differences in the final energy differences.

Using the $1/X^3$ dependence of the residual correlation energy on the basis set size proposed by Helgaker et al.[26] we used the following, previously applied equation to obtain the CCSD(T) energies of the systems in the infinite basis set limit: $E_\infty = E_{\text{HF/cc-pVQZ}} + 64/37E_{\text{correl/cc-pVQZ}} - 27/37E_{\text{correl/cc-pVTZ}}$ with the basis set held constant at cc-pVDZ on part II. For the CCSD and CCSD(T) calculation of the NO bond dissociation energy, a counterpoise correction for basis set superposition error (BSSE) was included. Poor or no convergence of the coupled-cluster equations were obtained in many cases when using Hartree−Fock reference orbitals; accordingly, the coupled-cluster expansion was instead performed using Kohn−Sham orbitals obtained using the B3LYP functional, leading to better convergence and much smaller singles excitation amplitudes.[27] The "HF" energy used in the extrapolation scheme is accordingly not the true HF energy, but instead the energy of the reference determinant formed from the Kohn−Sham orbitals. We do not include any thermal or zero-point energy corrections; these are small for the spin-state splittings and should decrease the bond energies by 1−2 kcal/mol. Geometries are provided in Supporting Information.

3. Results and Discussion

3.1. DFT Results on Heme Systems. In the present study, we consider the addition of NO to two heme systems with different oxidation states of the central iron atom, FeP(SH) and FeP(Im), where P denotes a porphyrin ring. In FeP(SH) (see Figure 1) the iron is in the +3 oxidation state. The same FeP(SH)[28−30] species and the related FeP(SCH_3)[31] have been the object of many previous computational studies, as they can be considered simple models of the thiolate-ligated heme group which is commonly found in cytochrome P450s and other hemoproteins. In FeP(Im), the iron porphyrin is ligated to imidazole, resulting in a +2 oxidation state of the iron. This system has also been investigated computationally[1,2,5] as it is a good model of histidine-ligated Fe(II) porphyrins found in the active site of many enzymes, e.g., in myoglobin. The aim of this study is to obtain reliable predictions of the bond energy for both systems, which in turn requires an accurate value for the relative energy of the different spin states of FeP(SH) and FeP(Im).

Due to the availability of already published calculated geometrical data on both systems and because our results are comparable to them, the structures are not discussed here, but some details are provided in Table S2 in the Supporting Information. Our DFT results on the relative energies (Table 1) of the various spin states of FeP(Im) are in accordance with previous results.[3,5,32] B3PW91 predicts a quintet ground state while with B3LYP the triplet state lies slightly lower, with the quintet very slightly higher in energy. Both functionals predict the singlet state to lie significantly higher in energy. The BP86 functional overestimates the stability of the low and intermediate spin species, leading to a prediction that the ground state is low spin for both systems, in disagreement with experiment. We would like to note that in this study we assumed (as was also done, e.g., by Spiro et al.[33]) that the FeP(Im) system adopts a C_s symmetrical structure. This assumption was motivated by convenience and by the fact that our previous study on the different isomers of FeP(Im) showed that the energy difference between C_s and non-C_s structures is very small.[5]

TABLE 1: Relative DFT/BS I Energies (kcal/mol) of Different Species [Fe]-X, Where [Fe] Is FeP(SH) or FeP(Im) and X Is Nothing or NO

	system	B3PW91	B3LYP	BP86
FeP(SH)	^{2}[Fe]	4.8	1.6	−15.2
	^{4}[Fe]	4.4	1.6	−8.0
	^{6}[Fe]	0.0	0.0	0.0
	^{1}[Fe−NO][a]	−4.0	−2.7	−49.1
FeP(Im)	^{1}[Fe]	9.0	4.3	−12.9
	^{3}[Fe]	2.5	−0.5	−10.5
	^{5}[Fe][b]	0.0	0.0	0.0
	^{2}[Fe-NO][a]	−11.7	−14.1	−50.8

[a] The relative energy is calculated with respect to the energies of the separated high-spin Fe complexes and the NO ligand. [b] Calculated in the ^{5}A′ state.

The FeP(SH) system has a sextet ground state according to the B3PW91 and B3LYP results. The energies of the lowest lying doublet and quartet states are predicted to be very similar and are close to the sextet state. This result is similar to those obtained in an earlier study,[32] but with the OPBE functional a larger difference between the energies of the doublet (1.9 kcal/mol) and quartet states (4.2 kcal/mol) has been obtained.[29]

Concerning the NO adducts, we only consider those binding modes of NO to the heme systems in which the nitrogen end of NO binds to the iron, as previous studies showed that this is favored over the binding by the oxygen end of the molecule.[5] Furthermore, we only study the lowest lying spin state for the NO complexes: the singlet for FeP(SH) and the doublet for FeP(Im). Table 1 shows the relative energies of the NO complexes, with details of the structures provided in Table S2 in the Supporting Information. We simply note here that bonding of NO to the heme models results in a shortening of the axial Fe−S or Fe−N bonds, and in the decrease of the iron−porphyrin nitrogen bond lengths. NO binds in an almost linear fashion to Fe(III) in FeP(SH), with an FeNO angle of 170°. This is frequently explained in the same manner as CO binding to Fe(II) hemes, as [Fe^{II}CO] and [Fe^{III}NO] systems are isoelectronic, with a total of six electrons in the d orbitals of the metal and π^* orbitals of the ligand. This leads to a singlet ground state for these species. However, the bonding between Fe(II) hemes and NO involves seven electrons, and the overlap between the empty d_{z^2} orbital of the metal and the half-occupied π^* orbital of the NO determines the FeNO bond angle. At small angles the overlap is more favorable, which leads to an FeNO angle of about 140° in the Fe(II) systems in general and in (FeP(Im)). The bent Fe−NO geometry has been suggested to be of functional importance for the storage and transport of the NO molecule.[34]

The bond energy of NO to ferric FeP(SH) is predicted to be very small, of only 4 and 2.7 kcal/mol by the B3PW91 and B3LYP functionals, respectively. For ferrous FeP(Im), the calculated NO bond energies are about 10 kcal/mol higher: 11.7 kcal/mol with B3PW91 and 14.1 kcal/mol with the B3LYP functional. However, all of these bond energies are very low when compared with experiment and show the same discrepancies as noted before.[6,17] For example, experiments show that the heat of NO binding to P450cam is about −19 kcal/mol.[8] In contrast to B3LYP and B3PW91 the pure BP86 functional predicts a very large bond energy, relative to the high-spin heme

fragment, of about 50 kcal/mol for both FeP(Im) and FeP(SH). This is partly due to the fact that this functional does not predict the correct spin state ordering for the pentacoordinate fragments and instead predicts low-spin ground states for both systems. Nevertheless, the very different behavior of this functional compared to the hybrid functionals remains when one considers "adiabatic" bond energies with no major change in spin at the metal. The bond dissociation energies for NO release from the FeP(SH) and FeP(Im) adducts leading to doublet FeP(SH) and singlet FeP(Im), respectively, are 33.9 and 37.8 kcal/mol with the BP86 functional, respectively. In contrast, B3LYP predicts values of 4.3 and 18.4 kcal/mol, respectively, and B3PW91 gives values of 8.8 and 20.7 kcal/mol. We report results for some other functionals in Table S1 in the Supporting Information; many of these other functionals reproduce either the problems associated with the spin state ordering or those associated with the bond energies discussed here for the B3LYP, B3PW91, and BP86 functionals. One functional, HCTH407,[35] seems to perform better, however, and it has been reported elsewhere[17] that OLYP gives reasonable results for ferrous heme systems. Our focus is however not on which functional gives the best results but rather on showing that many commonly used functionals produce a poor description of some or all relative energies in these systems.

3.2. DFT Results on Model Systems. The above work suggests that B3LYP and B3PW91 functionals may strongly underestimate the bond energy of NO to both ferrous and ferric heme systems, while the pure BP86 functional strongly overestimates it. Therefore there is a need to calibrate DFT results to more accurate methods. The simple heme models considered above are too large to be studied by accurate ab initio methods, such as CCSD(T) in conjunction with large basis sets. Therefore, we have to use model systems to calibrate our DFT results (Figure 2). One of the ways to reduce the size of the system and to keep its most important characteristics is to use two chelating amidine ligands instead of the porphyrin ring.[5,36−38] The chelating amidines exhibit some of the main features of the porphyrin ring: the overall charge and the binding mode of the nitrogen ligands is exactly the same, but instead of one single aromatic porphyrin ring there are two separated ring systems. Figure 2. shows the structure of the model systems. Models **1** and **2** ($[Fe(C_nH_{n+2}N_2)_2SH]$ where $n = 1$ or 3) are Fe(III) systems with an SH ligand as in FeP(SH). Model **3** $[Fe(C_1H_3N_2)_2NH_3)]$ is an Fe(II) system which includes ammonia as the fifth axial ligand of the iron center. This is an improvement over our previous study of a related Fe(II) heme model, in which H_2O was used as the axial ligand.[5]

All three model systems were confined to C_s symmetry in our calculations, and in order to obtain a geometry as similar to the porphyrin ring as possible, atoms of the amidine ligands were constrained to lie in a single plane during geometry optimization. The iron atom was however free to move, at least within the symmetry plane defining the C_s symmetry of the system.

In Table 2. we present the relative energies of the different spin states of the model systems and that of the NO-bound complexes. In the case of the smaller models (**1** and **3**) the B3LYP and B3PW91 functionals strongly favor the higher spin states. This is not surprising in the case of model **3**, as in our previous work with H_2O as axial ligand we observed a similar phenomenon.[5] Indeed, the fact that a somewhat similar spin state splitting is computed for model **3** in this study as was obtained for the related model with H_2O as axial ligand in our previous work[5] suggests that both systems give meaningful results.

TABLE 2: Relative DFT/BS I Energies (kcal/mol) of Different Species [Fe]−X, Where [Fe] Is Model 1, Model 2, or Model 3 and X Is Nothing or NO

	system	B3PW91	B3LYP	BP86
model **1**	^{2}[Fe]	26.4	22.8	10.3
	^{4}[Fe]	9.3	7.2	−2.1
	^{6}[Fe]	0.0	0.0	0
	^{1}[Fe−NO][a]	5.5	6.7	−38.7
model **2**	^{2}[Fe]	−5.2	−7.0	−28.4
	^{4}[Fe]	−2.3	−4.2	−14.3
	^{6}[Fe]	0.0	0.0	0.0
	^{1}[Fe−NO][a]	−2.5	−0.5	−48.3
model **3**	^{1}[Fe]	30.9	25.1	14.8
	^{3}[Fe]	14.8	12.0	2.0
	^{5}[Fe]	0.0	0.0	0.0
	^{2}[Fe−NO][a]	1.4	−0.2	−40.2

[a] Compared to the energies of the separated fragments.

Although the nature of the axial ligand (H_2O or NH_3) apparently only has a minor effect on the spin state splittings of these systems, there is a systematic difference that should perhaps be noted.[39] All functionals obtain similar quintet−triplet splittings for model **3** (e.g., 12.0 kcal/mol with B3LYP) and the related water complex (e.g., 10.7 kcal/mol, also with B3LYP, see ref 5). The quintet−singlet splitting is however smaller with the ligand ammonia in species **3** (e.g., 25.1 kcal/mol with B3LYP) than with the water ligand (e.g., 31.3 kcal/mol with B3LYP, see ref 5). This difference can be explained by considering the nature of the occupied orbitals. For both the triplet and quintet states, the d_{z^2} orbital which interacts with the ammonia or water donor ligand is singly occupied, whereas in the singlet state it is empty. The singlet state is therefore somewhat less unstable relative to the quintet and triplet states with the better ammonia ligand.

For the Fe(III) model **1**, the higher spin states are also strongly favored with the hybrid functionals, with the calculated splitting between sextet, quartet, and doublet states rather similar to the splitting obtained between quintet, triplet, and singlet states for model **3**. The B3PW91 functional predicts the largest energy gap between the sextet and doublet states. It should be noted that both model **1** and model **3** differ somewhat in the key features of the geometry around the iron center from what is observed for a full porphyrin ligand. In the latter, all four NFeN angles are approximately equal, at 90° when the iron atom is in the plane of the ligand. In the amidine ligands of models **1** and **3**, the chelating nitrogen atoms have a small bite angle, leading to very different NFeN angles when considering N atoms on the same ligand and on different ones. In the optimized low-spin state structures of models **1** and **3**, the NFeN angles are of about 113° and 67°. These values mean that the ligand field and the orbital splittings in the model are rather different from those found in the full porphyrin system.

In this respect, model **2** is significantly closer to the real system as the vinylogous amidine ligands permit a larger bite angle, with NFeN angles of 88.6° and 90.2°, thus very close to the ideal values. The calculated energy splittings between the different spin states (Table 2) are accordingly much smaller, closer to the situation found for the porphyrin ring (Table 1). In contrast to what was found for the latter, though, where the sextet was predicted to be the ground state with hybrid functionals, with the doublet and quartet states slightly higher in energy, model **2** is predicted to have a doublet ground state with both hybrid functionals, with the quartet also lying lower in energy than the sextet, but with relatively small energy gaps.

TABLE 3: Relative HF, CCSD, and CCSD(T) energies (in kcal/mol) of different species [Fe]-X, where [Fe] is model 1, 2, or 3 and X is nothing or NO[a]

		basis set (Fe/amidines)									
		cc-pVTZ/cc-pVDZ			cc-pVQZ/cc-pVDZ			cc-pVTZ/cc-pVTZ			cc-pV∞Z/ cc-pVDZ
	system	HF	CCSD	CCSD(T)	HF	CCSD	CCSD(T)	HF	CCSD	CCSD(T)	CCSD(T)
model **1**	^{2}[Fe]	102.7	52.5	37.8	102.8	48.5	33.2	103.3	53.9	38.5	29.8
	^{4}[Fe]	61.7	28.3	18.8	61.7	25.7	16.0	62.4	30.0	20.4	13.9
	^{6}[Fe]	0	0	0.0	0.0	0.0	0.0	0.0	0.0	0.0	0.0
	^{1}[Fe-NO]	224.5	55.0	1.9 (7.5)	224.2	49.4	−4.7 (0.4)	223.7	55.7	1.4 (*c*)	−9.3 (−4.5)
model **2**	^{2}[Fe]	101.9	22.9	0.6	101.7	18.6	−4.1	*b*	*b*	*b*	−7.4
	^{4}[Fe]	55.2	17.3	7.4	55.1	14.6	4.3	*b*	*b*	*b*	2.2
	^{6}[Fe]	0.0	0.0	0.0	0.0	0.0	0.0	*b*	*b*	*b*	0.0
	^{1}[Fe-NO]	222.0	44.7	−10.7	*b*	*b*	*b*	*b*	*bb*	*b*	*b*
model **3**	^{1}[Fe]	96.4	46.4	37.2	95.7	42.6	32.9	*c*	*c*	*c*	30.4
	^{3}[Fe]	65.0	28.7	21.8	64.5	26.2	19.0	*c*	*c*	*c*	17.3
	^{5}[Fe]	0.0	0.0	0.0	0.0	0.0	0.0	*c*	*c*	*c*	0.0
	^{2}[Fe-NO]	178.3	36.7	−3.6 (1.6)	178.7	32.7	−8.7 (−4.0)	*c*	*c*	*c*	−12.7 (−8.3)

[a] Results are shown for several basis set combinations on the metal and NO, and the spectator ligands, and for CCSD(T) results extrapolated to the infinite basis set limit. The BSSE corrected CCSD(T) energy of the NO complexes is given in parentheses. [b] Calculations too large to be feasible. [c] Calculation not carried out.

With the BP86 functional, lower spin states are also much more favored with model **2** than with model **1**.

Turning to the bond energies of the NO complexes, BP86 predicts a much larger bond energy for all systems than the hybrid functionals, as was observed for the full iron porphine systems FeP(Im) and FeP(SH). Indeed, for model **1**, both hybrid functionals predict the NO complex to be higher in energy than the separated fragments, whereas very small positive or negative bond energies are obtained for models **2** and **3**. The bond energies calculated for the NO complexes of model **2** and FeP(SH) are very similar in the case of the three functionals, which supports our previous observation that the electronic structure of model **2** reasonably mimics that of FeP(SH).

3.3. CCSD(T) Calculations on Model Systems. These results are presented in Table 3. However, before we discuss these results and before we compare them to the DFT results of section 3.2, we would like to note that the accuracy of CCSD(T) results is not completely known. Similar calculations on main-group compounds with well-defined single-reference behavior would yield relative energies to within 1−3 kcal/mol or better. However it is often considered that single-reference methods such as CCSD(T) are not reliable for transition metal compounds such as those studied here because correlation of compact doubly occupied metal d orbitals and of weak metal−ligand bonding electron pairs tends to require a multireference description. We note that coupled-cluster methods, especially CCSD(T) due to its inclusion of many of the effects of triple excitations, actually give rather good results even in borderline multireference systems.[40]

There is some evidence of multireference character in our calculations, foremost the fact that convergence of the coupled-cluster expansion for the NO complexes was difficult or impossible when using Hartree−Fock reference orbitals. For cases where convergence could be achieved, several of the singles and doubles CCSD amplitudes were very large. For the results presented here, we however used Kohn−Sham orbitals as reference orbitals for the CCSD(T) calculations. The Kohn−Sham orbitals give much improved convergence, and also tend to resemble Brueckner orbitals in the sense that they minimize the contribution of single excitations in the CCSD expansion.[27] In cases where it is possible to get converged results with both HF and KS orbitals, it has been found that the CCSD(T) total energy is rather similar for the two cases,[27] but the KS-based results can be superior in cases of borderline convergence as found here. With the KS reference, the CCSD(T) calculations on the NO complexes are much better behaved and, e.g., include small to medium T_2 amplitudes only, suggesting that the species studied here should be well described by single-reference methods. The cases with the largest T_2 amplitudes, the model **1** and **2** NO adducts, have largest T_2 amplitudes of ca. 0.1, much smaller than the values of up to 0.2−0.3 obtained for species such as MgO or O_3 that are reasonably well described by CCSD(T).[41]

It is well-known that larger basis sets are necessary to obtain reliable energies with CCSD(T) and that it is desirable to extrapolate to the infinite basis limit, generally based on calculations with triple- and quadruple-ζ basis sets.[19,26] Unfortunately, even the model systems treated here are too large for description with quadruple-ζ basis sets, so some compromises need to be made in order to carry out basis set extrapolation. We used smaller basis sets on the amidine and NH_3 or HS ligands than on the Fe−NO core. In order to test this approximation, and assess the effect of the basis set size on the amidine ligands on the relative energies of different spin states, we calculated the CCSD(T) energies of model **1** spin states with three different basis set combinations (see Table 3). These results show that the quality of the basis set on iron influences the spin-state energies of systems to a much larger extent than the size of the basis set on the amidine ligands. Relative HF, CCSD, and CCSD(T) energies obtained with cc-pVTZ/cc-pVDZ and cc-pVTZ/cc-pVTZ basis set combinations are very similar. Therefore for the other systems we only used the cc-pVTZ/cc-pVDZ and cc-pVQZ/cc-pVDZ basis set combinations. Extrapolation to the infinite basis set limit based on these results appears to be well behaved and produces results that should be accurate to within a few kcal/mol.

In our earlier work, we had no problems with CCSD(T) convergence when using Hartree−Fock reference orbitals for the pentacoordinate heme models and the CO and H_2O adducts and, accordingly, did not use KS-CCSD(T).[5] Here, we were required to use Kohn−Sham reference orbitals for all species due to convergence problems with the NO adducts when using HF orbitals. It can be seen from Table 3 that this change in procedure does not alter the calculated spin-state splittings significantly. As noted in section 3.2, the calculated B3LYP quintet/triplet splitting for model **3** (12.0 kcal/mol) is almost

the same as that obtained for the very similar species in the previous study (10.7 kcal/mol, see ref 5). This similarity is also found in the CCSD(T) values (17.3 kcal/mol here, for model **3** at the extrapolated cc-pV∞Z/ cc-pVDZ basis limit, vs 16.7 in the earlier work). The trend for the quintet/singlet splitting is also preserved. This shows that the use of KS orbitals does not lead to inconsistencies with the earlier work.

Let us turn now to the CCSD(T) results for the model system and to a comparison between these and the corresponding DFT values. Note that as part of the CCSD(T) calculations, we carry out B3LYP calculations using the large correlation-consistent basis sets used for the coupled-cluster calculation. Relative energies in these calculations are very similar to those obtained with BS I and are not discussed but are available in Table S3 of the Supporting Information. In our first calibration test we compare the relative energies of the different spin states of the three model systems with CCSD(T). The effect of correlation (HF vs CCSD and CCSD(T)) is very large, as in our earlier study, and even the effect of triples is very significant. The effect of extending the basis set on the Fe and NO centers is also large, so use of large basis sets and extrapolation to the infinite basis limit is important. As stated above, we believe that the estimated infinite basis set CCSD(T) values should be quite accurate.

These values lead to predicted high-spin ground state sextet and quintet for models **1** and **3**, respectively, and close-lying sextet, quartet, and doublet states (with the latter lowest in energy) for model **2**. Comparing these benchmark results to the earlier DFT values, it is obvious that hybrid functionals perform much better than the pure BP86 functional in reproducing these results, as already anticipated by comparison to experiment for the full heme model. BP86 overestimates the stability of the low and intermediate spin states relative to the high-spin states by about 20 kcal/mol for all three models. The spin state ordering of the three models, as found by CCSD(T), is predicted correctly by the hybrid functionals, the only exception is the quartet state of model **2**, which is predicted to be higher in energy than the doublet by CCSD(T) but lower with DFT. The B3PW91 functional performs the best in calculating the spin state splittings of the model systems: all relative energies agree to within better than 4 kcal/mol with the CCSD(T)/cc-pV∞Z,cc-pVDZ results.

The CCSD(T) bond energies for NO are also rather sensitive to correlation and to basis set, so care is needed to reach benchmark quality ab initio values for these important quantities. When comparing the DFT and CCSD(T) NO bond energies for the model systems, we always consider the calculated bond energy relative to the high-spin state of the fragment (sextet or quintet). This is done even when the calculations do not predict the high-spin state to be the ground state, as this provides a better comparison to the full porphyrin systems. Due to the size of model **2**, extrapolated CCSD(T)/cc-pV∞Z,cc-pVDZ results are only available for models **1** and **3**. Increasing the basis set on Fe and NO from cc-pVTZ to cc-pVQZ increases the bond energy by 5−6 kcal/mol for models **1** and **3**, and in the CCSD(T)/cc-pV∞Z,cc-pVDZ limit leads to a bond energy of 9.3 kcal/mol for model **1** and of 12.7 kcal/mol for model **3**. Including the counterpoise correction for basis set superposition error (BSSE) reduces these values to 4.5 and 8.3 kcal/mol, respectively. For model **2**, computational limitations restrict us to the cc-pVTZ/cc-pVDZ basis set combination; assuming a similar contribution of larger basis sets and of BSSE, one can estimate a bond energy for NO in this case of ca. 16 kcal/mol. In comparison, the B3PW91 values in Table 2 for models **1**−**3** are of −5.5, 2.5, and −1.4 kcal/mol. It appears therefore that B3PW91 underestimates the bond energy for all of these systems, including Fe(III) (models **1**, **2**) and Fe(II) (model **3**) centers, by about 10 kcal/mol.

Taking this correction factor into account, and using the data in Table 1, it can be seen that the "correct" NO bond energy in the case of the FeP(SH) and FeP(Im) models should be of the order of 15 and 20 kcal/mol, respectively. These values are much closer to the experimental values than those calculated with the hybrid functionals directly. It is not useful to compare calculated values directly with experimental ones, as no experiments address the particular porphyrin models described here: protein systems[7−9] involve additional hydrogen bonding or involve dissociation of ligands prior to NO bonding, and the gas phase models[11,12] do not include a proximal imidazole or SH^- ligand. However, the heat of reaction with pentacoordinate Fe(III) in camphor-bound cytochrome P450 is 20 kcal/mol, quite close to the 15 kcal/mol estimated here for binding of NO, especially bearing in mind the absence of the protein environment in our study.

One aspect that is worth considering is why the hybrid functionals underpredict the bond energies by so much, as understanding this may be helpful when exploring other ligand binding processes using DFT. Several comments are in order here. First, it has been suggested that the effect of including exact exchange in hybrid DFT functionals is to correct in part for the spurious self-interaction of one electron with itself in standard functionals.[42] However, using 100% exact exchange does not lead to good results, partly because the self-interaction effects, despite their nonphysical nature, can act as proxies for an important physical effect, namely, medium-range electron correlation as is, e.g., found in "left−right" correlation of electrons in a bonded pair. In this light, including a proportion of exact exchange serves to tune the degree of error due to self-interaction and the importance of medium-range correlation effects. In some bonding environments, where medium-range correlation is in some sense "standard", the typical 20% contribution of exact exchange found in functionals such as B3LYP will lead to favorable error cancelation and hence yield good results. In other cases, e.g., where medium-range correlation is more important, these functionals may underestimate bonding energies.

This insight has been developed into a highly accurate empirical model for correcting calculated energies with a given functional, by using parameters based on the degree of medium-range correlation found for a given bonding pattern.[43] This approach has also been applied to transition metal compounds,[44] where at least in some cases fairly large correction terms of close to 10 kcal/mol are needed. It appears that the binding of NO to iron centers, not studied in that paper, is a case where the required correction factor would be even larger. This interpretation is consistent with one aspect of the calculations: the large T_2 amplitudes mentioned above for the bound NO species all correspond to excitation of two electrons from a metal d orbital of π symmetry with respect to the Fe−NO axis into the corresponding NO π^* vacant orbital. This type of excitation clearly corresponds to description of the left−right correlation associated with back-bonding from the metal to the π^* orbitals of the ligand, and it is perfectly reasonable to assume that hybrid functionals underestimate the degree of correlation associated with this bonding.

On the basis of this analysis, one might expect functionals with a smaller degree of exact exchange to perform better in terms of predicting the NO bond energy. At first sight, this is

not the case: as can be seen in Table 1, BP86 grossly overpredicts the bond energy. However, this is in great part due to this functional being unable to predict the correct spin-state splitting in the NO-free fragment. If one adds the appropriate B3PW91 spin-state splittings to the BP86 bond energies calculated with respect to the low-spin fragments, one obtains predicted bond energies of 28.1 and 29 kcal/mol for FeP(SH) and FeP(Im), respectively. These are now larger that the corresponding correct values, suggesting that BP86 does not make the same type of error as the hybrid functionals but instead exaggerates the effects of medium-range correlation.

Conclusions

In this paper we compared DFT and CCSD(T) results on the spin states of various models of Fe(II)− and Fe(III)−heme systems and on the bonding of NO to these systems. The DFT results for large models of the heme system show that of the studied DFT functionals only hybrid functionals can correctly predict the ground spin state of the pentacoordinate metal fragment, with the "pure" BP86 GGA functional greatly overestimating the low-spin states. The DFT methods we have used here were not intended to be exhaustive; we are aware that other functionals exist and may give better results for the properties of interest. For example, we are aware that in the case of other iron systems the pure OLYP functional was shown to give good description of the spin-state energetics.[45] However, the functionals used here, B3LYP, B3PW91, and BP86, among the most commonly used functionals for the description of bonding of NO to heme groups, perform badly with respect to describing the NO bond energies. There are also indications that this is a case where it will be difficult to obtain a single functional that provides accurate results for *all* the key energetics, as the B3LYP and B3PW91 functionals describe the spin-state splitting in the five-coordinate heme system quite well but the intrinsic bond energy of NO poorly, whereas BP86 described the splitting poorly but the bonding somewhat better.

Reduced-size models of the full porphyrin system are used to calibrate the DFT methods. Geometrical and energetic considerations show that the enlarged model **2** is a good representation of the heme system, but this model is very computationally demanding with respect to CCSD(T) calculations. The smaller models **1** and **3** are reasonable models of the full system. Coupled-cluster calculations with extrapolation to the infinite basis limit confirm that the hybrid functionals perform well for calculating the spin-state energetics. For the NO bond energy, these calculations confirm that the hybrid functionals underestimate the strength of binding both to the Fe(III) models and the Fe(II) system. With these results as a reference, the estimated bond energies of NO to FeP(SH) and FeP(Im) systems are 15 and 20 kcal/mol, respectively. A discussion of the origin of the underbinding by the hybrid functionals concludes that these functionals do not account well for the medium-range correlation contribution to bonding in the Fe−N system, most likely due to problems describing the π back-bonding from filled metal d orbitals to the π^* orbitals of NO.

Acknowledgment. J.O. acknowledges receipt of an EU Marie Curie Fellowship (Project "Modelling CYPs").

Supporting Information Available: Tables of relative energies, properties, Cartesian coordinates, and DFT energies for the studied systems. This material is available free of charge via the Internet at http://pubs.acs.org.

References and Notes

(1) Siegbahn, P. E. M.; Blomberg, M. R. A. *Chem. Rev.* **2000**, *100*, 421–437.
(2) Spiro, T. G.; Zgierski, M. Z.; Kozlowski, P. M. *Coord. Chem. Rev.* **2001**, *219*, 923–936.
(3) Harvey, J. N. *J. Am. Chem. Soc.* **2000**, *122*, 12401–12402.
(4) Harvey, J. N. *Faraday Discuss.* **2004**, *127*, 165–177. Strickland, N.; Mulholland, A. J.; Harvey, J. N. *Biophys. J.* **2006**, *90*, L27–L29.
(5) Strickland, N.; Harvey, J. N. *J. Phys. Chem. B* **2007**, *111*, 841–852.
(6) Blomberg, L. M.; Blomberg, M. R.A.; Siegbahn, P. E.M. *J. Inorg. Biochem.* **2005**, *99*, 949–958.
(7) (a) Wanat, A.; Wolak, M.; Orzel, L.; Brindell, M.; van Eldik, R.; Stochel, G. *Coord. Chem. Rev.* **2002**, *229*, 37–49. (b) van Eldik, R. *Coord. Chem. Rev.* **2007**, *251*, 1649–1662. (c) Brindell, M.; Stawoska, I.; Orze3, Ł; Łabuz, P.; Stochel, G.; van Eldik, R. *Biochim. Biophys. Acta* **2008**, *1784*, 1481–1492.
(8) Franke, A.; Stochel, G.; Jung, C.; van Eldik, R. *J. Am. Chem. Soc.* **2004**, *126*, 4181–4191.
(9) Franke, A.; Stochel, G.; Suzuki, N.; Higuchi, T.; Okuzono, K.; van Eldik, R. *J. Am. Chem. Soc.* **2005**, *127*, 5360–5375.
(10) Franke, A.; Hessenauer-Ilicheva, N.; Meyer, D.; Stochel, G.; Woggon, W.-D.; van Eldik, R. *J. Am. Chem. Soc.* **2006**, *128*, 13611–13624.
(11) Chen, O. N.; Groh, S.; Liechty, A.; Ridge, D. P. *J. Am. Chem. Soc.* **1999**, *121*, 11910–11911.
(12) Angelelli, F.; Chiavarino, B.; Crestoni, M. E.; Fornarini, S. *J. Am. Soc. Mass Spectrom.* **2005**, *16*, 589–598.
(13) For some examples, see: Crespo, A.; Martí, M. A.; Kalko, S. G.; Morreale, A.; Orozco, M.; Gelpi, J. L.; Luque, F. J.; Estrin, D. A. *J. Am. Chem. Soc.* **2005**, *125*, 4433–4444. Capece, L.; Estrin, D.; Marti, M. A. *Biochemistry* **2008**, *47*, 9416–9427.
(14) Sigfridsson, E.; Ryde, U. *J. Inorg. Biochem.* **2002**, *91*, 101–115. (a) Chen, H.; Ikeda-Saito, M.; Shaik, S. *J. Am. Chem. Soc.* **2008**, *130* (44), 14778–14790. (b) Marti, M. A.; Crespo, A.; Capece, L.; Boechi, L.; Bikiel, D. E.; Scherlis, D. A.; Estrin; D.A., *J. Inorg. Biochem.* **2006.**, *100*, 761–770.
(15) Tangen, E; Svadberg, A.; Ghosh, A. *Inorg. Chem.* **2005**, *44*, 7802–7805.
(16) Rovira, C.; Kunc, K.; Hutter, J.; Ballone, P.; Parrinello, M. *J. Phys. Chem. A* **1997**, *101*, 8914–8925.
(17) Radoñ, M.; Pierloot, K. *J. Phys. Chem. A* **2008**, *112*, 11824–11832.
(18) See e.g.: Praneeth, V. K. K.; Paulat, F.; Berto, T. C.; George, S. D.; Näther, C.; Sulok, C. D.; Lehnert, N *J. Am. Chem. Soc.* **2008**, *130*, 15288–15303.
(19) Helgaker, T.; Ruden, T. A.; Jorgensen, P.; Olsen, J.; Klopper, W. *J. Phys. Org. Chem.* **2004**, *17*, 913.
(20) Ghosh, A.; Taylor, P. R. *Curr. Opin. Chem. Biol.* **2003**, *7*, 113–124.
(21) *Jaguar, version 6.0*, Schrödinger, LLC, New York, 2005.
(22) Amos, R. D.; Bernhardsson, A.; Berning, A.; Celani, P.; Cooper, D. L.; Deegan, M. J. O.; Dobbyn, A. J.; Eckert, F.; Hampel, C.; Hetzer, G.; Knowles, P. J.; Korona, T.; Lindh, R.; Lloyd, A. W.; McNicholas, S. J.; Manby, F. R.; Meyer, W.; Mura, M. E.; Nicklass, A.; Palmieri, P.; Pitzer, R.; Rauhut, G.; Schutz, M.; Schumann, U.; Stoll, H.; Stone, A. J.; Tarroni, R.; Thorsteinsson T. and Werner, H.-J. *MOLPRO*, a package of ab initio programs designed by H.-J. Werner and P. J. Knowles,version 2002.3; University of Birmingham, U.K., 2002.
(23) de Jong, W. A.; Harrison, R. J.; Dixon, D. A. *J. Chem. Phys.* **2001**, *114*, 48–53.
(24) Dunning, T. H. *J. Chem. Phys.* **1989**, *90*, 1007–1023.
(25) Balabanov, N. B.; Peterson, K. A. *J. Chem. Phys.* **2005**, *123*, 064107.
(26) Helgaker, T.; Klopper, W.; Koch, H.; Noga, J. *J. Chem. Phys.* **1997**, *106*, 9639–9646.
(27) For the use of Kohn−Sham orbitals in coupled-cluster calculations, see: Harvey, J. N.; Aschi, M. *Faraday Discuss.* **2003**, *124*, 129–143. Beran, G. J. O.; Gwaltney, S. R.; Head-Gordon, M. *Phys. Chem. Chem. Phys.* **2003**, *5*, 2488–2493.
(28) Meunier, B.; de Visser, S. P.; Shaik, S. *Chem. Rev.* **2004**, *104*, 3947–3980.
(29) Groenhof, A. R.; Swart, M.; Ehlers, A. W.; Lammertsma, K. *J. Phys. Chem. A* **2005**, *109*, 3411–3417.
(30) Shaik, S.; Kumar, D.; de Visser, S. P.; Altun, A.; Thiel, W. *Chem. Rev.* **2005**, *105*, 2279–2328.
(31) Rydberg, P.; Sigfridsson, E.; Ryde, U. *J. Biol. Inorg. Chem.* **2004**, *9*, 203–223.
(32) Ogliaro, F.; de Visser, S. P.; Shaik, S. *J. Inorg. Biochem.* **2002**, *91*, 554–567.
(33) Kozlowski, P. M.; Spiro, T. G.; Zgierski, M. Z. *J. Phys. Chem. B* **2000**, *104*, 10659–10666.
(34) Maes, E. M.; Roberts, S. A.; Weichsel, A.; Montfort, W. R. *Biochemistry* **2005**, *44*, 12690–12699.

(35) Boese, A. D.; Handy, N. C. *J. Chem. Phys.* **2001**, *114*, 5497–5503.
(36) Maseras, F. *New J. Chem.* **1998**, *22*, 327–332.

(37) Siegbahn, P. E. M.; Blomberg, M. R. A. *Annu. Rev. Phys. Chem.* **1999**, *50*, 221–249.
(38) Newton, J. E.; Hall, M. B. *Inorg. Chem.* **1984**, *23*, 4627–4632.

(39) We thank one of the referees for pointing out this trend.

(40) Watts, J. D.; Urban, M.; Bartlett, R. J. *Theor. Chim. Acta* **1995**, *90*, 341–355.

(41) Karton, A.; Rabinovitch, E.; Martin, J. M. L.; Ruscic, B. *J. Chem. Phys.* **2006**, *125*, 144108.

(42) Cremer, D. *Mol. Phys.* **2001**, *99*, 1899. (a) Polo, V.; Kraka, E.; Cremer, D. *Mol. Phys.* **2002**, *100*, 1771. Polo, V.; Grafenstein, J.; Kraka, E.; Cremer, D. *Theor. Chem. Acc.* **2003**, 109–22.
(43) Friesner, R. A.; Knoll, E. H.; Cao, Y. X. *J. Chem. Phys.* **2006**, *125*, 124107.
(44) Rinaldo, D.; Tian, L.; Harvey, J. N.; Friesner, R. A. *J. Chem. Phys.* **2008**, *129*, 164108.
(45) Ganzenmüller, G.; Berkaïne, N.; Fouqueau, A.; Casida, M. E.; Reiher, M. *J. Chem. Phys.* **2005**, *122*, 234321. Pierloot, K.; Vancoillie, S. *J. Chem. Phys.* **2008**, *128*, 034104.

JP811316N